

Porous $\text{MnFe}_2\text{O}_4@\text{SiO}_2$ magnetic glycopolymer: A multivalent nanostructure for efficient removal of bacteria from aqueous solution

Javad Malakootikhah^a, Ali Hossein Rezayan^{a,*}, Babak Negahdari^{b,*}, Simin Nasseri^{c,d}, Hossein Rastegar^e

^a Department of Life Science Engineering, Faculty of New Sciences & Technologies, University of Tehran, Tehran, Iran

^b Department of Medical Biotechnology, School of Advanced Technologies in Medicine, Tehran University of Medical Sciences, Tehran, Iran

^c Center for Water Quality Research (CWQR), Institute for Environmental Research (IER), Tehran University of Medical Sciences, Tehran, Iran

^d Department of Environmental Health Engineering, School of Public Health, Tehran University of Medical Sciences, Tehran, Iran

^e Cosmetic Products Research Center, Iran Food and Drug Administration, Ministry of Health and Medical Education, Tehran, Iran

ARTICLE INFO

Keywords:

Glycoparticles

Bacteria

Ferrite

Saccharide

Magnetic separation

ABSTRACT

The focuses of this research is to prepare an efficient magnetic glycopolymer for bacteria removal from aqueous solution. To perform this idea; porous $\text{MnFe}_2\text{O}_4@\text{SiO}_2$ was functionalized with glucose and or maltose as an anchors to adhere onto bacteria cell surface. Aminopropyltriethoxysilane was employed to link the saccharides on magnetic nanoparticle surface. The hybrid materials were characterized with XRD, VSM, FT-IR, FESEM, TEM, zeta potential measurement and elemental mapping. Microscopic image showed that MnFe_2O_4 is in cluster form composed from tiny nanoparticles. After saccharide functionalization hybrid composite generate hyper-cross-linked porous structure as a result of polysilicate formation due to hydrolysis of silica source. *Escherichia coli* and *Bacillus subtilis* were selected as sample pathogens to evaluate the bacteria capturing ability of the magnetic glycopolymer. At the optimum conditions (pH = 6, time of 20 min, dosage of 15 mg) removal efficiency was more than 99% using both saccharide.

1. Introduction

In recent decades, it is considered to be one of the major needs of our modern society to explore an economically efficient technique for isolation/detection of pathogens (Chockalingam et al., 2010). This theme originates from the well-known threat of increase of antibiotic resistance of bacterial pathogens which causes bacteraemia, meningitis and respiratory tract infections of millions of people all over the world (Hartmann et al., 2012). Two main categories of widely distributed bacterial pathogens in nature include Genus *Bacillus* as a heterogenic group of gram-positive and gram-negative *Escherichia coli*. Due to endospore-forming abilities of *Bacillus*, these bacteria tolerate adverse conditions better than the nonsporulating bacterial and may proliferate in a wide range of environments including water and foods. Moreover, this pathogen is capable to produce enterotoxins and emetic toxin (From et al., 2005). *E. coli* contamination is also of concern to the food industry because it is found in the environment and is prevalent in domestic farm animals. Thus, potential cross-contamination at the farm, in meat processing plants, swimming pool and drinking water can lead to infections by *E. coli* (Infections et al., 2013; Weimer et al., 2001).

Above mentioned remarks are good stimulus to design new anti-bacterial and antifungal agents with better activity profiles and lower toxicity, alternative to well known conventional techniques (Iconaru et al., 2012).

The progress in the field of nanoscale science and engineering develops new research on materials to answer the yet unsolved problems in various areas such as environment, medicine, biology, chemistry, and electronics (Karao' et al., 2011). In consequence, nanomaterials or nanovectors are widely attracted great attention to their optical, mechanical and magnetic properties for biomedical applications including disease diagnosis and treatment (Huo et al., 2006). In especial case of biomedical applications, multifunctional nanomaterials have been employed considerably as potential platforms for bacteria sensing and separation. Some of various organic and inorganic employed nanomaterials in antibacterial systems include: zinc oxide (Copia et al., 2012; Popa et al., 2016), chitosan (Kong et al., 2010), mixed oxide (Ma et al., 2015a) graphene oxide (Ma et al., 2015b), $\text{g-C}_3\text{N}_4$ (Ma et al., n.d.) and alumina (Mu et al., 2015). Despite worthiness of these developed treatment process; efficient isolation or elimination of bacteria for water disinfection, food decontamination, and biotechnological

* Corresponding authors.

E-mail addresses: ahrezayan@ut.ac.ir (A.H. Rezayan), b-negahdari@sina.tums.ac.ir (B. Negahdari).

<https://doi.org/10.1016/j.ecoenv.2018.09.086>

Received 6 January 2018; Received in revised form 12 September 2018; Accepted 20 September 2018

Available online 28 September 2018

0147-6513/ © 2018 Published by Elsevier Inc.

applications is still a challenging task today.

Recently, magnetic nanoparticles (NPs) have been studied intensively in bioimaging, magnetic separation, hyperthermia therapy, targeted drug delivery, and catalysis (Shemirani and Beyki, 2015). Among the many magnetic NPs studied thus far, ferrite NPs especially MnFe_2O_4 shows remarkable characteristics, such as high thermal stability, which makes it applicable over a wide temperature range (Beyki et al., 2016). Like all naked magnetic NPs, manganese ferrite suffers from lack of sufficient stability and moderate bacterial capture efficiency hence modifying magnetic nanoparticles to improve its performance is inevitable (Wei et al., 2011). It seems that carbohydrates are good candidates for increase bacterial removal efficiency of magnetic NPs. In other words nanoparticles functionalized with carbohydrates presented a highly efficient interaction with bacteria lectins (Rezaei-Zarchi et al., 2012). Based on this merit several works were developed for bacteria capturing based on magnetic carbohydrates or glyconanoparticles (Iu et al., 2011). Basically, there are several types of glyconanoparticles, including metallic, semiconductor, magnetic and self-assembled structures with different forms including vesicles, micelles, nanoparticles and nanofibers (Yilmaz and Becer, 2015). Glycopolymers, synthetic macromolecules with sugar moieties, are other types of glyconanoparticles present high local concentrations of ligands on a small surface (Kiessling et al., 2006). Polymeric glyconanoparticles are synthesized with various backbone using cyclodextrine (Zhang et al., 2014), styrene and methacrylate (Slavin et al., 2011) and protein conjugate (Kiessling et al., 2006).

The development of inorganic polymers is a new promising technology that may be used in many applications (Simonsen et al., 2009). Among inorganic polymers, increasing interest in recent decades has been focused on silica-supported organic–inorganic hybrid materials because of their low cost, very stable and non-swelling characteristics (He et al., 2017). Ease of synthesis along with well-known surface chemistry due to presence of O, N, and S groups provide wonderful modification opportunities for the covalent attachment of appropriate organic molecules (Li et al., 2016). The synthesis of silica-supported polymers is normally carried out by hydrolysis of organosilanes combined with a sol–gel processing (Fan et al., 2014). Due to relatively high loading capacities, the polymer surface can be further modified through grafting reaction between amino/silanol groups with variety of functional groups (Cen et al., 2017).

Based on the mentioned merits and as a part of our interest in the synthesis of nanomaterials and investigation of their application in diagnosis, treatment and environmental remediation (Malakootikhah et al., 2017; Bagdeli et al., 2016; Taheri et al., 2016) in the present work magnetic glycopolymer was synthesized by immobilization of glucose and or maltose onto amino $\text{MnFe}_2\text{O}_4 @ \text{SiO}_2$ surface. Aminopropyltriethoxysilane (APTES) and tetraethylorthosilicate (TEOS) were condensed to prepare hyper-crosslinked polysilicate structure. Prepared magnetic glycopolymer was employed for capturing of bacillus and *E. coli* as sample pathogens. Moreover, effective parameters on capturing efficiency such as pH, contact time and glycopolymer dosage were studied and discussed in details. The efficiency of the method for bacteria capturing from real samples was also studied with treatment of sea water, fruit juice, river water, and milk samples.

2. Experimental

2.1. Materials and instruments

APTES, TEOS, $\text{Fe}(\text{NO}_3)_3 \cdot 9\text{H}_2\text{O}$, $\text{Mn}(\text{NO}_3)_2 \cdot 4\text{H}_2\text{O}$, sodium hydroxide, maltose, glucose and NH_3 (25%) were purchased from Merck (Darmstadt, Germany). Ethanol was supplied from Bidestan Company (Qazvin–Iran).

The prepared glycopolymers were characterized by Fourier transform infrared (FT-IR), Vibration sample magnetometer (VSM), Transmission electron microscopy (TEM), Field emission scanning

electron microscopy (FESEM), Elemental mapping, Thermal gravimetric analysis (TGA), Zeta potential measurements and Powder X-ray diffraction analysis (XRD). FT-IR were recorded with Attenuated total reflectance (ATR) method using Equinox 55, Bruker. VSM and TEM results were recorded with Lake Shore Model 7400 (Japan) and Zeiss-EM10C instruments. Elemental mapping and FESEM was recorded with Sigma VP instrument (Zeiss). TGA data were collected with a TA-Q-50 instrument. Zeta potentials of 0.1 g L^{-1} of glyconanoparticles were measured at varied pH conditions using Zetasizer Nano ZS90 (Malvern Instruments, U.K). A digital pH-meter (model 692, Metrohm, Herisau, Switzerland) was used for pH adjustment. XRD (X'Pert PRO, with Cu K α radiation at $k = 1.540589 \text{ \AA}$) was used to investigate the crystallinity of the glycoparticles.

2.1.1. Synthesis of MnFe_2O_4 magnetic nanoparticles

Coprecipitation method was applied for synthesis of MnFe_2O_4 magnetic nanoparticles. For this purpose, 7.00 g of $\text{Fe}(\text{NO}_3)_3 \cdot 9\text{H}_2\text{O}$ and 1.70 g of $\text{Mn}(\text{NO}_3)_2 \cdot 4\text{H}_2\text{O}$ were dissolved in 200 mL of distilled water. The mixture was then sonicated to yield a pellucid solution. When the temperature of the sonication bath reached to 80°C , 20.0 mL of NaOH solution (5.00 M) was added to the mixture immediately. Afterward, the resultant mixture was maintained in the same condition for 30 min. Next, it was cooled down to room temperature, filtered and washed with distilled water several times. At the end, the obtained black powder was dried at 80°C for 2 h.

2.1.2. Synthesis of silica coated ferrite ($\text{MnFe}_2\text{O}_4 @ \text{SiO}_2$) nanoparticles

To prepare silica coated ferrite, the magnetite ferrite (1.0 g) was first dispersed in 80 mL of water-ethanol mixture (1:3 v/v) by ultrasonic vibration for 15 min, and then concentrated aqueous ammonia (3.0 mL, 25 wt%) was added and stirred for 30 min. After that, 1.0 mL of TEOS diluted in ethanol (20 mL) was added dropwise to this dispersion and after stirring for 12 h, the obtained product was collected by magnetic separation, washed three times with ethanol and dried at 80°C for 2 h.

2.1.3. Synthesis of saccharide functionalized $\text{MnFe}_2\text{O}_4 @ \text{SiO}_2$ glycopolymer

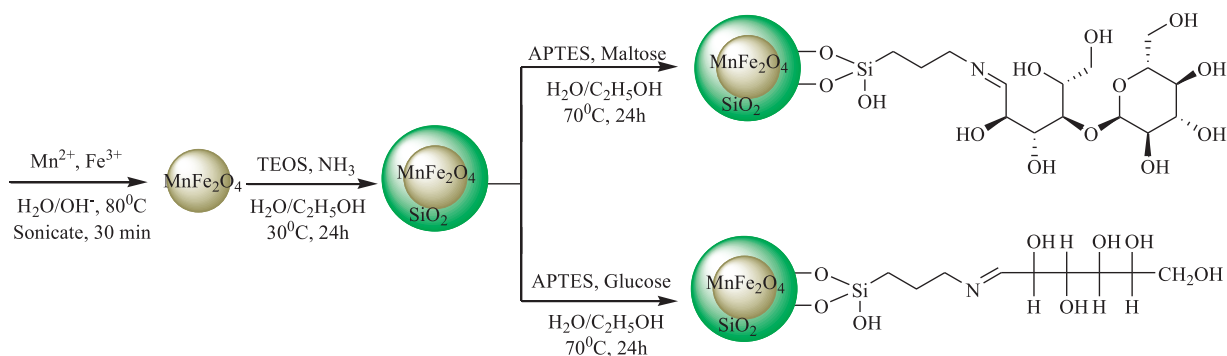
To prepare saccharide modified nanoparticles, 1.0 g of silica coated ferrite nanoparticles were ultrasonically dispersed in 70 mL of ethanol for 5 min. Then 0.77 g of glucose in 10 mL of distilled water was added to ferrite suspension, and then 1.0 mL of APTES in 10 mL ethanol was dripped to the nanoparticle – glucose mixture and refluxed at 70°C for 24 h along with magnetic stirring. After cooling to room temperature the glyconanoparticles were collected with magnetic field and washed with ethanol once and distilled water three times and dried at 60°C for 12 h. Same protocol was employed to prepare maltose modified ferrite nanoparticles. Amount of APTES and maltose were 1.0 mL and 1.54 g, respectively. Synthetic protocol is illustrated at Scheme 1.

2.2. Bacteria preparation

Gram-positive strain, *B. subtilis* and gram-negative *E. coli*, supplied from Institute Pastor, Tehran, Iran, were selected to evaluate bacteria capturing efficiency of prepared glyco – system. The bacteria were cultivated in 100 mL of Luria Broth growth (15 g L^{-1} tryptone, 5 g L^{-1} bacto-yeast extract, and 5 g L^{-1} NaCl) and shacked in an incubator at 30°C for 32 h. The cells were collected by centrifugation (4000g for 10 min at 4°C) and after washing the bacterial pellets with 0.9% of NaCl at pH 7.0, collected cells were then re-suspended in the mentioned physiological saline to obtain cell density of 1.5×10^8 Colony Forming Unit (CFU) per mL.

2.3. Bacteria capture experiment

Bacterial capturing studies were performed in sterilized physiological saline by dispersing 20 mg of glyco-particles in the 20 mL bacterial solutions with concentration of $1.5 \times 10^8 \text{ CFU mL}^{-1}$. After incubation



Scheme 1. Synthetic protocol for preparing glyconanoparticles.

in a shaker for 20 min the magnetic particles were separated from the suspension by using an external magnetic field. 1.0 mL of supernatant was collected and analyzed via filter membrane method. The parallel experiments were performed in absence of glyco-particles and average of triplicate experiment was selected to calculate removal percentage (%R):

$$\%R = 100 \times (CFU_0 - CFU_t) / CFU_0 \quad (1)$$

where CFU₀ and CFU_t are initial cell numbers and the number of colonies in the supernatant after collection of glyco-particles, respectively (El-boubbou et al., 2007).

3. Results and discussion

3.1. Characterization of the materials

EDX analysis was used to verify component of glycopolymers. Results showed that the pattern goodly exhibits all components of the materials. Weight percentages are shown at Fig. 1. It can be seen that carbon and nitrogen as well as silicium are presence with good density at the polymer structure. Moreover, it was found that the magnetic

fragments of glycopolymer i.e, manganese and iron are also presence in composite structure.

The XRD analysis (Fig. S1) was employed to verify the crystalline structure of as synthesized MnFe₂O₄ and Maltose modified MnFe₂O₄. In the XRD pattern of MnFe₂O₄ a typical main peaks of a cubic spinel structure are observable at 2θ = 29.64, 35.12, 42.48, 52.72, 56.2 and 61.76. These peaks can be assigned to (220), (311), (400), (422), (511), and (440) planes of ferrite nanoparticles. The modified nanoparticles was exhibited two main peaks at 2θ° equal to 10° and 22° which can be attributed to the (001) and (110) pseudo-orthorhombic reflections of the saccharide which can be ascribed to periodicity parallel to the maltose chain (Pouget et al., 1991). Moreover, characteristic peaks of the nanoparticles have been still appearing in the XRD spectrum of nanocomposite with high intensity which means that when maltose deposited on the surface of nanoparticles, the crystalline behavior of the ferrites is not hampered. Scherer equation was employed to determine the average crystallite size of MnFe₂O₄.

$$D = (0.9\lambda) / (\beta \cos\theta) \quad (2)$$

In this equation D is the average crystalline size, λ (0.1540589 nm) is the X-ray wavelength used, β (0.014) is the angular line width of half

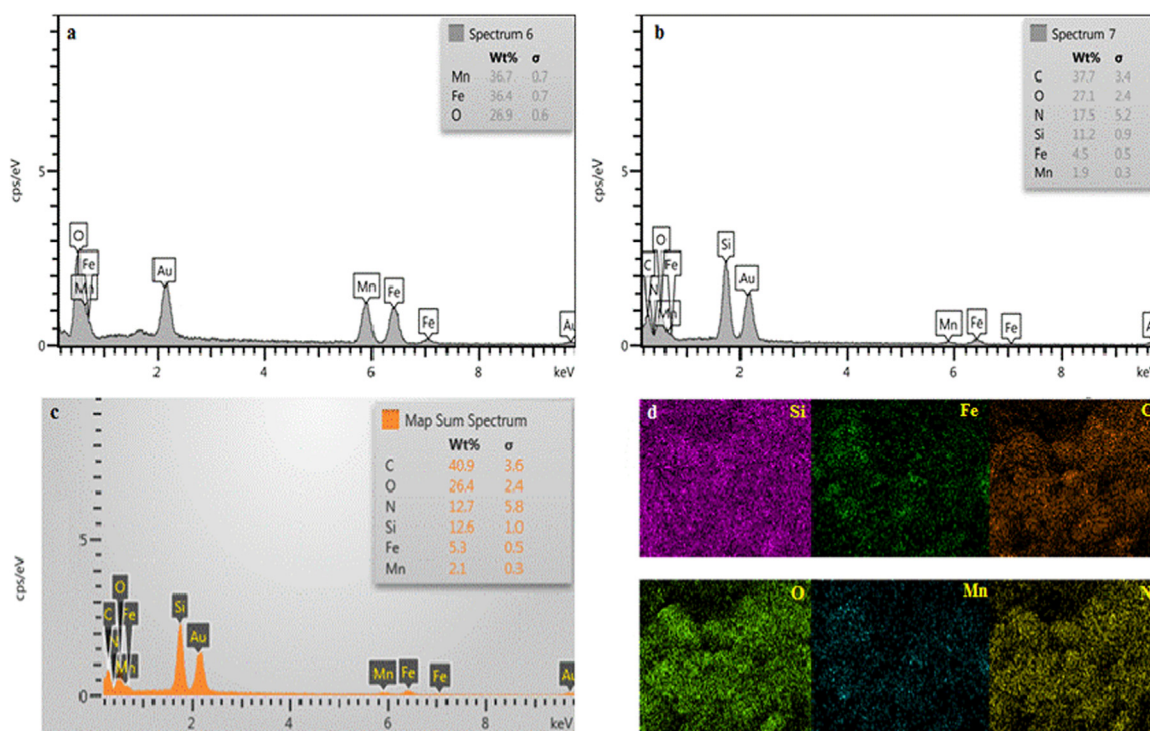


Fig. 1. EDX spectra of MnFe₂O₄ (a), glucose glycopolymer (b), maltose glycopolymer (c) and typical elemental mapping of maltose glycopolymer (d).

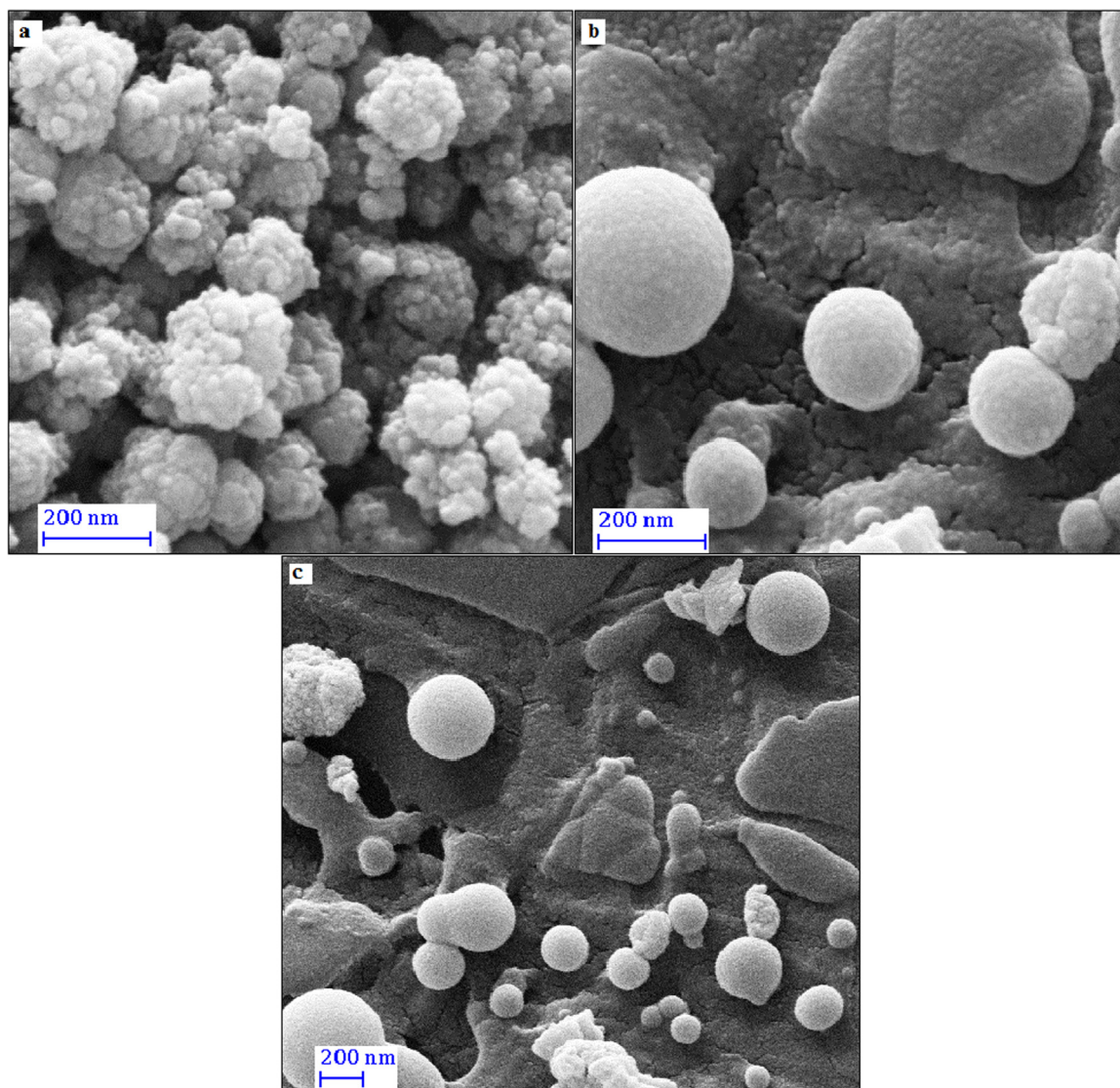


Fig. 2. FESEM images of MnFe₂O₄ (a), Maltose-glycopolymer (b) and glucose-glycopolymer (c), (Conditions: 1.0 mg composite coated with Au, number of image recording = 3).

maximum intensity in radians, and θ (17.56) is Bragg's angle expressed in degree (Shemirani and Beyki, 2015). According to this equation the average size of 10.4 nm was obtained for the nanoparticles.

FT-IR spectrums of MnFe₂O₄, MnFe₂O₄@TEOS, glucose-glycopolymer and maltose-glycopolymer are shown in Fig. S2. As can be seen ferrite spectra showed stretching vibration at 3400 cm⁻¹, 1625 cm⁻¹ and 573 cm⁻¹ corresponding to free and hydrogen bonded O-H, surface adsorbed water and octahedral and tetrahedral stretching vibration of Fe-O complexes, respectively. After modification with TEOS, new peak appeared at 1085 cm⁻¹ which can be assigned to Si-O groups. Glycopolymer also showed the peaks of manganese ferrite and TEOS coated magnetic nanoparticles along with new peaks corresponding to stretching of C-H and C-O as well as the OH bending vibration of primary alcoholic groups (Cai et al., 2015). The absorption peaks related to the C-H stretching and C-O-C pyranoid ring appeared at 2982 cm⁻¹ 1400 cm⁻¹. The C=N vibrations of an imines group also observed at 1631 cm⁻¹.

Fig. S3 shows TGA curves of MnFe₂O₄, MnFe₂O₄@TEOS, glucose-glycopolymer and maltose-glycopolymer as a function of temperature under argon atmosphere. As can be seen there is no significant weight loss in the curve of MnFe₂O₄, MnFe₂O₄@TEOS as the losing is 5.2% and 10.7%, respectively. This change probably is due to desorption of

physical adsorbed solvent such as water and ethanol. The curve of glucose-glycopolymer and maltose-glycopolymer showed main weight losing of 26.32 and 30.43 between 200 and 600 °C due to the dehydroxylation as well as decomposition of carbohydrate and organic structures grafted on glycopolymer surface. This result confirmed that the saccharides are presence onto composite structure with high density moreover as synthesized glycopolymers have good thermal stability.

The magnetic hysteresis loops for the materials are shown in Fig. S4. Value of magnetic saturation (M_s) for MnFe₂O₄, MnFe₂O₄@TEOS, glucose-glycopolymer and maltose-glycopolymer is 28.19, 18.07, 11.22 and 10.89 emu g⁻¹. As can be seen the value of M_s was decreased after surface modification of the nanoparticles. This is owing to the disaffiliation of the coated layer on the total magnetization as well as a lower volume fraction of the MnFe₂O₄ nanoparticles relative to the total volume of the nanocomposite. The magnetic remnant (M_r) value for the particles is 0.32, 0.47, 0.33 and 0.40 emu g⁻¹, respectively. With low value of M_r it may be concluded that the particles have superparamagnetic or ferromagnetic properties. In other words, the ratio of M_r/M_s between 0 and 1 confirms paramagnetic property of the nanoparticles. According to results the ratio of M_r/M_s is 0.011, 0.026, 0.029 and 0.036 which rely in the mentioned range hence the materials exhibited paramagnetic behavior (Nonkumwong et al., 2015).

The N_2 adsorption-desorption isotherm for the prepared materials is shown in Fig. S5. As can be seen the curve show type H_3 isotherm with a minor hysteresis loop as a result of filling and emptying of the mesopores by capillary condensation (Bayat et al., 2015). Loops of this type represent non-rigid aggregates of plate-like particles as well as the pore network consists of macropores which are not completely filled with pore condensate. The BET surface area of the $MnFe_2O_4$ is $148.8 \text{ m}^2/\text{g}$. After modification of the nanoparticle surface with TEOS, glucose and maltose the surface area decreased to 33.0, 5.8 and $3.0 \text{ m}^2/\text{g}$, respectively. Observed results confirmed deposition of the employed materials on the surface of $MnFe_2O_4$. According to the pore-size data the materials are classified as mesopores compounds (Dabrowski, 2001) with pore diameter of 4.9, 4.7, 10 and 18 nm for $MnFe_2O_4$, TEOS, glucose and maltose modified nanoparticles, respectively. Moreover, it was found that the total pore volume of the $MnFe_2O_4$, TEOS, glucose and maltose modified nanoparticles is 0.18, 0.038, 0.014 and 0.014, respectively.

The TEM images of $MnFe_2O_4$ and $MnFe_2O_4$ – TEOS is shown at Fig. S6a and S6b, respectively. As can be seen the $MnFe_2O_4$ nanoparticles showed fine nanoparticles with diameter less than 10 nm. After modification with TEOS change in the particle size is observed as the particles size increased more than 10 nm.

Fig. 2 shows the FESEM image of $MnFe_2O_4$, glucose-glycopolymer and maltose – glycopolymer. It can be seen at Fig. 2a that manganese ferrite composed from nano-scale clusters with diameter between 100 and 200 nm however, the clusters are agglomeration of very fine nanoparticles with diameter of 20–30 nm. Cluster formation is owing to the intramolecular hydrogen bonds between distinct nanoparticles. In other words, surface hydroxyl groups of ferrite nanoparticles are organizes in a rather complex fashion where an extended intramolecular network of hydrogen bonds is indicated as the basis of cohesion between the nanoparticles. Fig. 2b and c show the FESEM image of the as-prepared magnetic glycopolymers. It indicated that the nanocomposite exhibited hyper-crosslinked structure with aggregated fine sphere like nanoparticles.

Fig. 3a and b show interaction of *E. coli* and *B. subtilis* with glucose-glycopolymer. As can be seen *E. coli* is presence on the glycopolymer structure as microspheres. *B. subtilis* is also presence as baculiform microstructure on the glycopolymer surface. This is owed to the attractive interaction as dominant force between the magnetic glycopolymer and bacteria. In other words, cell surfaces of bacteria have negative charges which attract positively charged glycopolymer.

3.2. Optimization effective factors on capturing

It is known that several factors such as solution pH, contact time and amount of nanocomposite can affect bacterial capture efficiency. Among the mentioned variables solution pH is a main factor since it can change both sorbate and sorbent surface characteristics. To understand the role of pH on bacteria removal efficiency, determine of surface charge of the glycopolymers and bacteria is helpful as a result zeta potential measurements for $MnFe_2O_4$ @TEOS, glucose-glycopolymer and maltose-glycopolymer was performed and the pattern was depicted at Fig. 4a. It can be seen that $MnFe_2O_4$ @TEOS surface has negative charge at pH higher than 3.5. This situation is observable for glucose-glycopolymer and maltose-glycopolymer at pH higher than 7.5 and 7.0. Besides *B. subtilis* and *E. coli* show isoelectric point of 1.6 and 3.5, respectively. This means that at the pH higher than the mentioned values cell walls of bacteria has negative charge. Based on the above mentioned merits solution pH was the first factor that has been optimized. To evaluate the effect of this parameter bacterial capture experiments were performed in the pH range of 2–8 with 20 mL of bacterial solution with initial concentration of $1.5 \times 10^8 \text{ CFU mL}^{-1}$. Glycopolymer dosage was 20 mg and contact time was 30 min. As it was indicated in Fig. 4b, both glycopolymers show same behavior for *B. subtilis* and *E. coli* capturing. In other words with increasing pH from 2 to 8, *E. coli* capture efficiency by maltose – glycopolymer and glucose – glycopolymer decreased from 92% and 88% to around 61% and 55% however, *B. subtilis* capturing efficiency didn't shown significant decrease by increase in pH as removal percentage was 100% in pH = 2 which reached to 98% at pH = 8. Generally with increase in solution pH removal percentage decreases which can be explained based on the zeta potential measurements described above. As can be seen, glycopolymers possess positive charge at the pH below 7 but based on potential value charge density decreases with increasing pH besides bacterium surface has negative charge which interact with glycopolymer surface through electrostatic attraction. With increasing pH up to 8 negative charge density on the bacterial cell surfaces increases but positive charge density on the sorbent surface decreases which induces lower adhesion forces hence removal percentage decreases by increase of solution pH (Denis et al., 2002). According to results capturing efficiency at pH = 8 is in good level however the glycopolymer surface has negative charge at this situation. This can be explained with the presence of glucose and maltose on the composite structure. These saccharides can react with lectin of most types of bacteria hence saccharide – lectin interaction has main role in high efficiency of glycopolymers at alkali conditions. Other reason which interpret good efficiency of both nanocomposites at

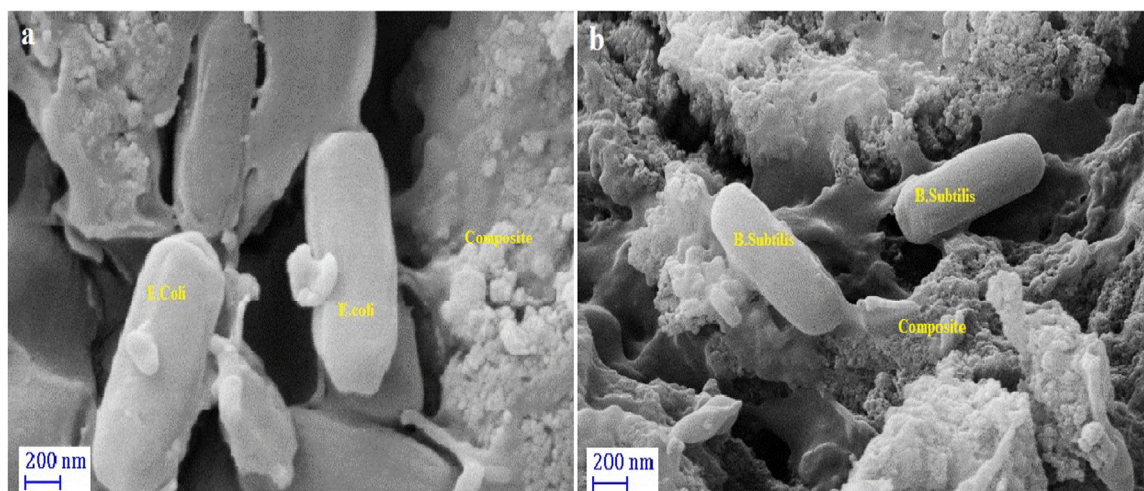


Fig. 3. *E. coli* (a) and *B. subtilis* (b) captured on the maltose – glycopolymer surface (Conditions: 1.0 mg collected composite after bacteria capturing, number of image recording = 3).

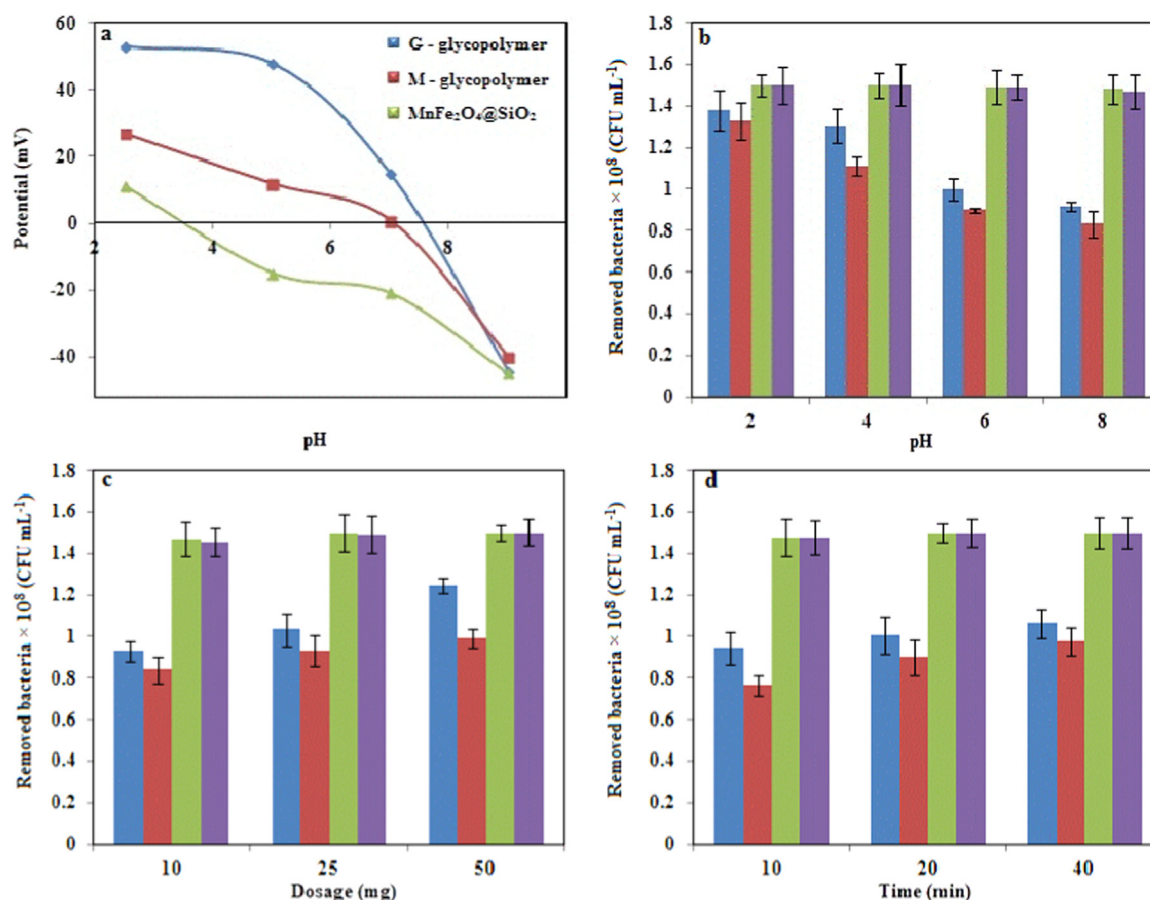


Fig. 4. Zeta potential measurements (a), Effect of pH (b), effect of dosage (c) and effect of time (d) on bacteria capturing (sample volume 20 mL, bacteria concentration 1.5×10^8 CFU mL⁻¹, n = 3, columns from left to right: Maltose – E.coli, Glucose – E.coli, Maltose – subtilis, Glucose – subtilis).

alkaline media is binding of deprotonated carboxylate groups with negatively charged on the bacteria surface with positive Fe and Mn ions through electrostatic interactions which induce the large adhesion force (Hossein Beyki and Fazli, 2017). Other reason for observed efficiency at alkali situation is the presence of hydrogen bonding as well as hydrophobic attraction causes adhesion of glycopolymers on the bacterial cell surfaces. The effects of glycopolymer dosage on bacterial capture (20 mL of 1.5×10^8 CFU mL⁻¹) were examined at three dosages level of 10, 25 and 50 mg and time of 20 min using *B. subtilis* and *E. coli* as model cells. According to results at Fig. 4c, with 10 mg of glucose – glycopolymer and maltose – glycopolymer, the *E. coli* capture efficiency was 56% and 62% which reached to 66% and 83% when the dosage increased to 50 mg. At the same situations the *B. subtilis* capture efficiencies increased from more than 97% to more than 99% by increase in dosage from 10 to 25 mg. However, the bacteria removal efficiencies obtained by maltose – glycopolymer were higher than those of glucose – glycopolymer. This could be attributed to the multivalent characteristic of maltose respect to glucose. In other words maltose could provide more accessible active binding points for bacterial capturing.

The effect of time to bacterial capture with initial concentration of 1.5×10^8 CFU mL⁻¹ was investigated at three times level of 10, 20 and 40 min with dosage of 20 mg at pH = 6 and the results were given in Fig. 4d. It was found that using the glycopolymers capture of *B. subtilis* occurs efficiently within first 10 min with capture efficiencies more than 98%. The cell removal efficiencies after 20 min reached to 100%. For *E. coli* capturing the efficiency was 51% and 63% in 10 min reaction that reached to 65% and 71% after 40 min then even after reaction with cells for 60 min, the capture efficiencies using not changed significantly. For further works the time of 20 min was selected as equilibrium time. Fast equilibrium can be explained with the fact that

kinetic of adsorption is governed by factors such as the interaction energy barrier and diffusivity (Gao et al., 2006). According to TEM results the glycopolymers have sheet – like porous structure these means that the sorbent exert multivalent effect on bacterial capture which confirmed presence of low energy barriers to be overcome before glycopolymer contact with the cells.

3.3. Recovery and reuse

Reusability of nanocomposite is a main factor which made the presented system more economic hence the recovery and reuse of glycopolymers throughout three consecutive bacteria capture/ regeneration cycles were examined with 20 mg of nanocomposites. 75% of ethanol/water solution was used as eluent. Ethanol selection is based on the fact that it can releases of bacteria from sorbent surface through decompose the bacteria cells walls. Results showed that by using glucose – glycopolymer the bacterial capture efficiencies were 100% at the first cycle which slightly decreased with increasing the regeneration cycles as reached to 97% and 94% in the second and third cycle. Whereas, maltose – glycopolymer showed higher efficiency as the capture efficiencies in the end of third cycle was more than 99%. In overall both glycopolymers exhibited good potential for repeated use to capture bacteria but maltose – glycopolymer has more efficiency owe to multivalent inherent of disaccharide maltose respect to glucose as a monosaccharide.

3.4. Bacteria capturing from orange juice and milk samples

The potential of presented system for bacteria capturing from real samples were examined with treatment of polluted orange juice and

milk samples. To perform the experiments 5 mL of sterilized orange juice and milk was added to the 15 mL of prepared bacterial solutions (1.5×10^8 CFU mL⁻¹) in physiological saline with pH of 6.0. After adding 20 mg of nanocomposite the mixture was incubated in a shaker for 20 min then the magnetic particles were separated from the suspension by using an external magnetic field. 1.0 mL of supernatant was collected and analyzed for bacterial concentration via filter membrane method. Results showed that subtilis removal efficiency from juice samples was 95% and 98.5% by using glucose – glycopolymer and maltose – glycopolymer, respectively. The capturing efficiency for milk sample was 99.5% by using both glycopolymer systems. These results proved the excellent performances of presented multifunctional glycopolymers for real samples treatment with complicated matrices.

3.5. Comparison glycopolymer performances

The performances of as synthesized glycopolymers for both gram negative and gram positive bacteria capturing was studied at the optimum level of variables (pH = 6, time 20 min and dosage of 20 mg). According to results by using glucose - glycopolymer and maltose – glycopolymer, *B. subtilis* capturing (initial concentration of 1.5×10^8 CFU mL⁻¹) was approximately complete at the mentioned optimum conditions. However the sorbents showed maximum efficiency of 67% for *E. coli* capturing at the optimum conditions. It was found that with increasing of adsorbent dosage and time up to 50 mg and 60 min, the *E. coli* capturing efficiency reached to 83%. These results confirmed that both glycopolymers have more efficiency for *B. subtilis* capturing relative to *E. coli*. The observed results can be explained based on two main factors which affect bacteria/solid surface interaction. A first reason for efficient *B. subtilis* capturing can be interpreted based on the bacteria cell wall. *E. coli* possesses an inner cytoplasmic membrane and outer membrane, and periplasmic space between the membranes contains one to two layers of peptidoglycan. In contrast, *B. subtilis* does not possess an outer membrane, but contain 10–20 layers of peptidoglycans modified by extensive anionic polymers (Sekiguchi and Yamamoto, 2012). In peptidoglycans, the glycan strands are made of disaccharide repeats, N-acetylglucosamine and N-acetylmuramic acid, which are linked by β -1,4-glycosidic bonds. The anionic polymers attached to vegetative peptidoglycans in *B. subtilis* are Lipoteichoic acid which is a high glycerol-phosphate-containing material that is anchored into the membrane by one end. The outer membrane of *E. coli* is a lipid bilayer which composed of glycolipids, principally lipopolysaccharide (LPS).

The LPS on the *E. coli* cell wall made it a hydrophobic surface. Besides it is known that the attachment of microbial cells to surfaces depends on the hydrophobicity of the cells. The more hydrophobic cells adhere more strongly to hydrophobic surfaces, while hydrophilic cells strongly adhere to hydrophilic surfaces (Krasowska and Sigler, 2014). Based on the explained items at the above; *E. coli* cell surface has hydrophobic characteristic besides *B. subtilis* surface has hydrophilic properties. The glycopolymers contain maltose and glucose which is hydrophilic compounds hence it can be estimates that they have more effective interaction with hydrophilic cell surface of *B. subtilis* besides the hydrophobic lipopolysaccharide (LPS) surface of *E. coli* accounts for the favored binding of it to a hydrophobic surface over hydrophilic surface (Yuan et al., 2017). Other reason for efficient *B. subtilis* capturing can be explained based on bacterial shape. Based on the TEM images at Fig. 2, *B. subtilis* has rod – like structure however *E. coli* has semi - spherical morphology hence *B. subtilis* should have been captured with more efficiency on the prepared porous glycopolymers. In other words attachment mechanisms would lead to preferential removal of long, rod-shaped cells. Some reports suggest that cell attachment to solid surfaces indeed may be greater for elongated cells than for spherical cells due to physical filtration mechanisms (Weiss et al., 1995).

4. Conclusions

An efficient bacterial capture system was developed based on glucose and maltose glycopolymers. Results showed that the magnetic glycopolymers have high efficiency (more than 99%) for *B. subtilis* removal. Moreover, the results confirmed multivalent effect of glycopolymers for efficient removing of bacteria. Effect of solution pH showed that at pH = 6, contact time of 20 min and dosage of 20 mg approximately complete removal can be achieved. Reuse of the capturing system showed that it has good reusability after three cycle of sorption and desorption. Moreover the sorbents showed good efficiency for bacteria removal from milk and orange juice samples.

Acknowledgments

This paper has been extracted from Ph.D. thesis. The authors would like to acknowledge the Iran National Science Foundation (INFS) (Project 90004726) and Tehran Urban Research and Planning Center for the financial support of this work. Also the authors wish to gratefully thank the Applied Chemistry Research Group, ACECR, Tehran University and Department of Environmental Health Engineering, School of Public Health, Tehran University of Medical Sciences for technical supports.

Appendix A. Supporting information

Supplementary data associated with this article can be found in the online version at doi:10.1016/j.ecoenv.2018.09.086.

References

- Bagdadi, Samira, Rezayan, Ali Hossein, Taheri, Ramezan Ali, Mehdi Kamali, M.H., 2016. FRET- based immunoassay using CdTe and AuNPs for the detection of OmpW antigen of *Vibrio cholerae*. Food Biosci. <https://doi.org/10.1016/j.neuroimage.2017.02.019>.
- Bayat, M., Beyki, M.H., Shemirani, F., 2015. One-step and biogenic synthesis of magnetic Fe3O4-Fir sawdust composite: application for selective preconcentration and determination of gold ions. J. Ind. Eng. Chem. 21, 912–919. <https://doi.org/10.1016/j.jiec.2014.04.032>.
- Beyki, M.H., Alijani, H., Fazli, Y., 2016. Solvent free synthesized MnFe2O4@polyamid resin as a novel green nanohybrid for fast removing Congo red. J. Mol. Liq. 216, 6–11. <https://doi.org/10.1016/j.molliq.2016.01.017>.
- Cai, Y., Zheng, L., Fang, Z., 2015. Selective adsorption of Cu(II) from aqueous solution by ion imprinted magnetic chitosan microspheres prepared from steel pickling waste liquor. RSC Adv. <https://doi.org/10.1039/C5RA16547D>.
- Cen, S., Li, W., Xu, S., Wang, Z., Tang, Y., 2017. Application of magnetic Cd2+ ion-imprinted mesoporous organosilica nanocomposites for mineral wastewater treatment. RSC Adv. 7, 7996–8003. <https://doi.org/10.1039/C6RA27679B>.
- Chockalingam, A.M., Kumar, H., Ramesh, R., Chittor, R., 2010. Gum arabic modified Fe3O4 nanoparticles cross linked with collagen for isolation of bacteria. J. Nanotechnol. 8, 30–39. <https://doi.org/10.1186/1477-3155-8-30>.
- Copcia, V.-E., Gradinaru, R., Mihai, G.-D., Bilba, N., Sandu, I., Platform, A.I., 2012. Investigation anti-bacterial effect of zinc oxide nanoparticles upon life of listeria monocytogenes. Ann. Biol. Res. 3, 3679–3685.
- Dabrowski, A., 2001. Adsorption from theory to practice. Adv. Colloid Interface Sci. 93, 135–224.
- Denis, A., Touhami, A., Dufre, Y.F., 2002. Probing microbial cell surface charges by atomic force franc. Langmuir 18, 9937–9941. <https://doi.org/10.1021/la026273k>.
- El-boubbou, K., Gruden, C., Huang, X., 2007. Magnetic glyco-nanoparticles: a unique tool for rapid pathogen detection, de- contamination and strain differentiation supporting information Kheirredine El-Boubbou. J. Am. Chem. Soc. 1–26. <https://doi.org/10.1021/ja076086e>.
- Fan, H., Liu, J., Yao, H., Zhang, Z., Yan, F., Li, W., 2014. Ionic imprinted silica-supported hybrid sorbent with an anchored chelating schiff base for selective removal of cadmium (II) ions from aqueous media. Ind. Eng. Chem. Res.
- From, C., Pukall, R., Schumann, P., Granum, P.E., 2005. Toxin-producing ability among bacillus spp. outside the bacillus cereus group. Appl. Environ. Technol. 71, 1178–1183. <https://doi.org/10.1128/AEM.71.3.1178>.
- Gao, D., Lin, D.Q., Yao, S.J., 2006. Protein adsorption kinetics of mixed-mode adsorbent with benzylamine as functional ligand. Chem. Eng. Sci. 61, 7260–7268. <https://doi.org/10.1016/j.ces.2006.07.013>.
- Hartmann, M., Betz, P., Sun, Y., Gorb, S.N., Lindhorst, T.K., Krueger, A., 2012. Saccharide-modified nanodiamond conjugates for the efficient detection and removal of pathogenic bacteria. Chem. A Eur. J. 18, 6485–6492. <https://doi.org/10.1002/chem.201104069>.
- He, H., Gan, Q., Feng, C., 2017. Preparation and application of Ni(II) ion-imprinted silica gel polymer for selective separation of Ni(II) from aqueous solution. RSC Adv. 7,

- 15102–15111. <https://doi.org/10.1039/C7RA00101K>.
- Hossein Beyki, M., Fazli, Y., 2017. Polyhydroxyquinoline-carbon nanotube chelating resin for selective adsorption of lead ions: multivariate optimization, isothermic, and thermodynamic study. *Res. Chem. Intermed.* 43. <https://doi.org/10.1007/s11164-016-2650-4>.
- Huo, Q., Liu, J., Wang, L., Jiang, Y., Lambert, T.N., Fang, E., 2006. A new class of silica cross-linked micellar core-shell nanoparticles. *J. Am. Chem. Soc.* 6447–6453.
- Iconaru, S.L., Motelica-Heino, M., Sizaret, Stanislas, Predoi, Daniela, 2012. Synthesis and characterization of polysaccharide-maghemite composite nanoparticles and their antibacterial properties. *Nanoscale Res. Lett.* 7, 576–584.
- Infections, O., Gould, L.H., Mody, R.K., Clogher, P., Cronquist, A.B., Garman, K.N., Lathrop, S., Medus, C., Spina, N.L., Webb, T.H., White, P.L., Wymore, K., Gierke, R.E., Mahon, B.E., Griffin, P.M., 2013. Increased recognition of Non-O157 shiga toxin – producing *Escherichia coli* infections in the United States. *Foodborne Pathog. Dis.* 10, 453–460. <https://doi.org/10.1089/fpd.2012.1401>.
- Iu, H.L., Ang, J.T., Uo, L.G., Ie, J.X., Ang, Y.W., 2011. Galactose-functionalized magnetic iron-oxide nanoparticles for enrichment and detection of ricin toxin. *Anal. Sci.* 27, 19–24. <https://doi.org/10.2116/analsci.27.19>.
- Karao, E., Kavas, H., Baykal, A., Toprak, M.S., 2011. Effect of hydrolyzing agents on the properties of poly (ethylene glycol) -Fe₃O₄ nanocomposite. *Nano Micro Lett.* 3, 79–85.
- Kiessling, L.L., Gestwicki, J.E., Strong, L.E., 2006. Synthetic multivalent ligands as probes of signal transduction. *Angew. Chem.* 2348–2368. <https://doi.org/10.1002/anie.200502794>.
- Kong, M., Chen, X.G., Xing, K., Park, H.J., 2010. Antimicrobial properties of chitosan and mode of action: a state of the art review. *Int. J. Food Microbiol.* 144, 51–63. <https://doi.org/10.1016/j.jfoodmicro.2010.09.012>.
- Krasowska, A., Sigler, K., 2014. How microorganisms use hydrophobicity and what does this mean for human needs? *Front. Cell. Infect. Microbiol.* 4, 1–7. <https://doi.org/10.3389/fcimb.2014.00112>.
- Li, W., He, R., Tan, L., Xu, S., Kang, C., 2016. One-step synthesis of periodic ion imprinted mesoporous silica particles for highly specific removal of Cd²⁺ from mine wastewater. *J. Sol-Gel Sci. Technol.* <https://doi.org/10.1007/s10971-016-3987-2>.
- Ma, S., Zhan, S., Jia, Y., Shi, Q., Zhou, Q., n.d. Enhanced disinfection application of Ag-modified g-C₃N₄ composite under visible light 186, 77–87.
- Ma, S., Zhan, S., Jia, Y., Zhou, Q., 2015a. Superior antibacterial activity of Fe₃O₄-TiO₂ nanosheets under solar light. *ACS Appl. Mater. Interfaces.* <https://doi.org/10.1021/acsami.5b06264>.
- Ma, S., Zhan, S., Jia, Y., Zhou, Q., 2015b. Highly efficient antibacterial and Pb(II) removal effects of Ag-CoFe₂O₄-GO nanocomposite. *ACS Appl. Mater. Interfaces.* <https://doi.org/10.1021/acsami.5b02209>.
- Malakootikhah, Javad, Rezayana, Ali Hossein, Negahdari, Babak, Simin Nasseri, H.R., 2017. Glucose reinforced Fe₃O₄/cellulose mediated amino acid: reusable magnetic glyconanoparticles with enhanced bacteria capture efficiency. *Carbohydr. Polym.* 170, 190–197.
- Mu, D., Mu, X., Xu, Z., Du, Z., Chen, G., 2015. Removing bacillus subtilis from fermentation broth using alumina nanoparticles. *Bioresour. Technol.* 197, 508–511. <https://doi.org/10.1016/j.biortech.2015.08.109>.
- Nonkumwong, J., Pakawanit, P., Wipatanawin, A., Jantaratana, P., Ananta, S., Srisombat, L., 2015. Synthesis and cytotoxicity study of magnesium ferrite-gold core-shell nanoparticles. *Mater. Sci. Eng. C.* <https://doi.org/10.1016/j.msec.2015.12.021>.
- Popa, C.L., Deniaud, A., Michaud-soret, I., Guégan, R., Motelica-heino, M., Predoi, D., 2016. Structural and biological assessment of zinc doped hydroxyapatite nanoparticles. *J. Nanomater.* 2016, 1–10.
- Pouget, J.P., Jozefowicz, M.E., Epstein, a.J., Tang, X., MacDiarmid, a.G., 1991. X-ray structure of polyaniline. *Macromolecules* 24, 779–789. <https://doi.org/10.1021/ma00003a022>.
- Rezaei-Zarchi, S., Imani, S., Mohammad Zand, A., Saadati, M., Zaghari, Z., 2012. Study of bactericidal properties of carbohydrate-stabilized platinum oxide nanoparticles. *Int. Lett.* 2, 21. <https://doi.org/10.1186/2228-5326-2-21>.
- Sekiguchi, J., Yamamoto, H., 2012. 4-3. Cell wall structure of *E. coli* and *B. subtilis*.
- Shemirani, F., Beyki, M.H., 2015. Dual application of facilely synthesized Fe₃O₄ nanoparticles: Fast reduction of nitro compound and preparation of magnetic poly-phenylthiourea nanocomposite for efficient adsorption of lead ions. *RSC Adv.* 5, 22224–22233. <https://doi.org/10.1039/c4ra12549e>.
- Simonsen, M.E., Sønderby, A.C., Søgaard, E.G., 2009. Synthesis and characterization of silicate polymers. *J. Sol-Gel Sci. Technol.* 50, 372–382. <https://doi.org/10.1007/s10971-009-1907-4>.
- Slavin, S., Burns, J., Haddleton, D.M., Becer, C.R., 2011. Synthesis of glycopolymers via click reactions. *Eur. Polym. J.* 47, 435–446. <https://doi.org/10.1016/j.eurpolymj.2010.09.019>.
- Taheri, R.A., Rezayan, A.H., Rahimi, F., Mohammadnejad, J., Kamali, M., 2016. Development of an immunosensor using oriented immobilized anti-OmpW for sensitive detection of *Vibrio cholerae* by surface plasmon resonance. *Biosens. Bioelectron.* 86, 484–488. <https://doi.org/10.1016/j.bios.2016.07.006>.
- Wei, Z., Zhou, Z., Yang, M., Lin, C., Zhao, Z., Huang, D., Chen, Z., Gao, J., 2011. Multifunctional Ag@Fe₂O₃ yolk-shell nanoparticles for simultaneous capture, kill, and removal of pathogen. *J. Mater. Chem.* 21, 16344. <https://doi.org/10.1039/c1jm13691g>.
- Weimer, B.C., Walsh, M.K., Beer, C., Koka, R., Wang, X., 2001. Solid-phase capture of proteins, spores, and bacteria. *Appl. Environ. Microbiol.* 67, 1300–1307. <https://doi.org/10.1128/AEM.67.3.1300>.
- Weiss, T.H., Mills, a.L., Hornberger, G.M., Herman, J.S., 1995. Effect of bacterial cell shape on transport of bacteria in porous media. *Environ. Sci. Technol.* 29, 1737–1740. <https://doi.org/10.1021/es00007a007>.
- Yilmaz, G., Becer, C.R., 2015. Glycopolymers and their interactions with lectins. *Polym. Chem.* 6, 55031–55514. <https://doi.org/10.1016/j.eurpolymj.2013.06.001>.
- Yuan, Y., Hays, M.P., Hardwidge, P.R., Kim, J., 2017. Surface characteristics influencing bacterial adhesion to polymeric substrates. *RSC Adv.* 7, 14254–14261. <https://doi.org/10.1039/C7RA01571B>.
- Zhang, Q., Su, L., Collins, J., Chen, G., Wallis, R., Mitchell, D.A., Haddleton, D.M., Becer, C.R., 2014. Dendritic cell lectin-targeting sentinel-like unimolecular glycoconjugates to release an Anti-HIV drug. *J. Am. Chem. Soc.*